Journal of Quantitative Spectroscopy & Radiative Transfer 158 (2015) 111–118

Contents lists available at ScienceDirect

Journal of Quantitative Spectroscopy & Radiative Transfer

journal homepage: www.elsevier.com/locate/jqsrt

Effect of polarization on dual-band infrared metamaterial emitters or absorbers

Atsushi Sakurai [a,b], Bo Zhao [a], Zhuomin M. Zhang [a,*]

[a] George W. Woodruff School of Mechanical Engineering, Georgia Institute of Technology, Atlanta, GA 30332, USA
[b] Department of Mechanical and Production Engineering, Niigata University, 8050, Ikarashi 2-no-cho, Niigata 950-2181, Japan

ARTICLE INFO

Article history:
Received 17 September 2014
Received in revised form
26 November 2014
Accepted 28 November 2014
Available online 8 December 2014

Keywords:
Absorptance
Emittance
Metamaterials
Nanostructures
Polarization effect

ABSTRACT

This work deals with the spectral radiative properties of metamaterials made of a 2D metallic pattern on a dielectric thin film that separates the top periodic structure from a metal ground plane. Two distinct patterns are considered: one consists of disconnected double-rectangle gold pattern and the other is made of L-shape pattern. Both structures exhibit dual-band emission or absorption peaks in the infrared region. Unlike the disconnected rectangular pattern for which the normal emittance is independent of the polarization angle, the L-shape structure shows strong polarization dependent due to near-field coupling. The electromagnetic fields at the resonant frequencies are analyzed using the finite-difference time-domain technique to elucidate the physical mechanisms accounting for the different behaviors. For both structures, the resonance mechanisms can be explained by magnetic polaritons. Inductor–capacitor circuit models are developed to quantitatively predict the resonance frequencies. This work helps the understanding of polarization dependence in metamaterials and may facilitate their applications in biosensing and infrared spectroscopic system.

1. Introduction

Electromagnetic metamaterials refer to a class of engineered artificial structures containing periodic patterns of (usually) metallic elements with geometric features smaller than the wavelength. Exotic and superior optical, thermal radiative, or microwave characteristics, which are absent or rarely exit in natural materials, have been demonstrated using metamaterials [1–3]. Recently, metamaterial emitters or absorbers with a metal–insulator–metal structure have attracted much attention [4–8]. Specifically, wavelength-selective infrared absorption or emission shows promising biosensing applications due to the infrared vibrational fingerprints of biomolecules that can be applied for their identification [9]. To meet the requirement for various applications, single-band, dual-band, and multi-band emitters and absorbers have been demonstrated. For example, polarization and angular insensitive near-perfect absorbers have been developed in the near infrared for plasmonic sensing with a single-band response [10]. Liu et al. [4] demonstrated dual-band and multi-band mid-infrared emitters using cross-shape patterns with different sizes. Zhang et al. [11] fabricated elliptical nanodisks, with a 90° rotation between two adjacent disks, to realize dual-band near-perfect absorption. Tao et al. [12] observed two absorption peaks in the far-infrared region based on the electric-field-coupled resonators. These metamaterial absorbers or emitters are designed for polarization-independent response. However, some metamaterial absorbers or emitters exhibiting polarization control ability are also attractive for practical applications where polarization selectivity is desired [13–17].

* Corresponding author.
E-mail address: zhuomin.zhang@me.gatech.edu (Z.M. Zhang).

http://dx.doi.org/10.1016/j.jqsrt.2014.11.018
0022-4073/

Although polarization-dependent radiative properties of asymmetric metamaterials have been observed [18–20], the near-field coupling in these structures has not been fully investigated. Further studies on the resonant mechanisms and coupling effects in metamaterial absorbers or emitters are necessary in order to better understand their polarization sensitivity to assist future design tailored toward specific applications.

The present study deals with two patterns that support magnetic resonances for dual-band emission or absorption peaks. A comparative study of the two metamaterial designs with different polarization dependences is performed. Both designs consist of a three-layer metamaterial structure with a metal (gold) pattern, a dielectric (Al_2O_3) film, and a gold ground plane. The difference lies in that unit cell of the top layer has different gold patterns. One of the structures is made of two separate gold rectangles and the other is constructed by connecting the two rectangles to form an L-shape pattern. The former structure shows polarization-independent radiative properties, while the latter exhibits strong polarization dependence. The objective of this study is to explore the underlying mechanisms that result in either polarization-dependent or polarization-independent radiative properties near the magnetic resonance or magnetic polariton (MP) wavelengths. The finite-difference time-domain (FDTD) technique is employed to calculate the radiative properties and the electromagnetic field distributions, which are then used to elucidate the resonance mechanism and to scrutinize the near-field coupling effect. Furthermore, the inductor–capacitor (LC) circuit model is developed for each structure considering the different geometries following the field distributions to quantitatively predict the MP frequencies.

2. Metamaterial structures and numerical method

Fig. 1 shows a unit cell of the double-rectangle and L-shape metamaterial emitters or absorbers. Gold patterns are placed over a dielectric film or spacer (Al_2O_3) on a ground plane made of a gold film that is thick enough to be treated as opaque. In the following, the rectangular pattern whose long side is along the y-direction is called the *vertical rectangle*, and the one along the x-direction is called the *horizontal rectangle*. The geometric parameters include period Λ, thickness of gold patterned layer h, thickness of dielectric layer d, long-side length w_1, short-side length w_2, and distances between the edge of the gold pattern and cell boundary s_1 and s_2. The parameters used for both metamaterial structures are listed in Table 1.

The FDTD method (Lumerical Solutions, Inc.) is used for calculating the infrared reflectance of the two metamaterial emitters and absorbers by solving the Maxwell equations. The optical constants of gold and Al_2O_3 are obtained from Palik [21]. For simplicity and ease of revealing the underlying mechanisms, the refractive index of Al_2O_3 is assumed to be constant according to $n=1.57$ at the wavelength $\lambda=6.25$ μm. In practice, Al_2O_3 becomes dispersive at wavelengths beyond 8 μm, resulting in a drop of the refractive index along with an increased absorption. Although the effect of the dispersive behavior should be taken into account for more realistic simulation, the focus of the present study is on elucidating the underlying mechanisms and therefore Al_2O_3 is treated as a lossless nondispersive dielectric. A unit cell of the considered structure is calculated using periodic boundary conditions

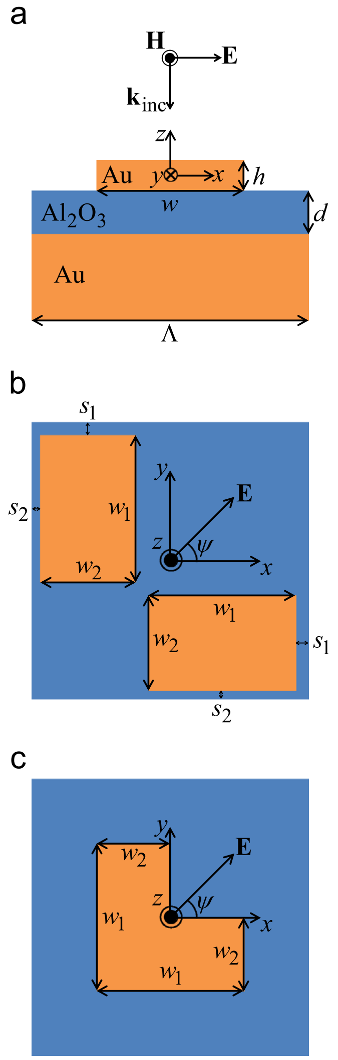

Fig. 1. Schematic of the metamaterial emitter and absorber. (a) Side view of the three-layer structure, also showing the incident wavevector $\mathbf{k}_{inc}$ and polarization angle; (b) top view of the double-rectangle pattern; (c) top view of the L-shape pattern. Note that gold (Au) is used for the metallic patterns and the ground plane, and Al_2O_3 is used for the dielectric film or spacer.

Table 1
Geometric parameters for the metamaterial structure used in the present study.

Period	Λ [μm]	3.2
Thickness of top metallic pattern	h [nm]	100
Thickness of dielectric spacer	d [nm]	140
Length of long side	w_1 [μm]	1.7
Length of short side of rectangle	w_2 [μm]	1.1
Length of short side of L-shape	w_2 [μm]	0.85
Length of margin	s_1 [μm]	0.15
Length of margin	s_2 [μm]	0.10